



## Original article

## Physiological cardiac hypertrophy: Critical role of AKT in the prevention of NHE-1 hyperactivity



Alejandra M. Yeves, María C. Villa-Abrille, Néstor G. Pérez, Andrés J. Medina, Eduardo M. Escudero, Irene L. Ennis\*

Centro de Investigaciones Cardiovasculares, Facultad de Ciencias Médicas, UNLP-CONICET, Argentina

## ARTICLE INFO

## Article history:

Received 10 April 2014

Received in revised form 28 August 2014

Accepted 6 September 2014

Available online 18 September 2014

## Keywords:

NHE-1

Physiological cardiac hypertrophy

AKT

IGF-1

Exercise training

## ABSTRACT

**Background:** The involvement of NHE-1 hyperactivity, critical for pathological cardiac hypertrophy (CH), in physiological CH has not been elucidated yet. Stimulation of NHE-1 increases intracellular  $\text{Na}^+$  and  $\text{Ca}^{2+}$  favouring calcineurin activation. Since myocardial stretch, an activator of NHE-1, is common to both types of CH, we speculate that NHE-1 hyperactivity may also happen in physiological CH. However, calcineurin activation is characteristic only for pathological hypertrophy. We hypothesize that an inhibitory AKT-dependent mechanism prevents NHE-1 hyperactivity in the setup of physiological CH.

**Methods:** Physiological CH was induced in rats by swimming (90 min/day, 12 weeks) or in cultured isolated cardiomyocytes with IGF-1 (10 nmol/L).

**Results:** Training induced eccentric CH development (left ventricular weight/tibial length:  $22.0 \pm 0.3$  vs.  $24.3 \pm 0.7$  mg/mm; myocyte cross sectional area:  $100 \pm 3.2$  vs.  $117 \pm 4.1$  %; sedentary (Sed) and swim-trained (Swim) respectively;  $p < 0.05$ ) with decreased myocardial stiffness and collagen deposition [ $1.7 \pm 0.05$  % (Sed) vs.  $1.4 \pm 0.09$  % (Swim);  $p < 0.05$ ]. Increased phosphorylation of AKT, ERK1/2, p90<sup>RSK</sup> and NHE-1 at the consensus site for ERK1/2-p90<sup>RSK</sup> were detected in the hypertrophied hearts (P-AKT:  $134 \pm 10$  vs.  $100 \pm 5$ ; P-ERK1/2:  $164 \pm 17$  vs.  $100 \pm 18$ ; P-p90<sup>RSK</sup>:  $160 \pm 18$  vs.  $100 \pm 9$ ; P-NHE-1  $134 \pm 10$  vs.  $100 \pm 10$ ; % in Swim vs. Sed respectively;  $p < 0.05$ ). No significant changes were detected neither in calcineurin activation [calcineurin A $\beta$   $100 \pm 10$  (Sed) vs.  $96 \pm 12$  (Swim)], nor NFAT nuclear translocation [ $100 \pm 3.11$  (Sed) vs.  $95 \pm 9.81$  % (Swim)] nor NHE-1 expression [ $100 \pm 8.5$  (Sed) vs.  $95 \pm 6.7$  % (Swim)]. Interestingly, the inhibitory phosphorylation of the NHE-1 consensus site for AKT was increased in the hypertrophied myocardium ( $151.6 \pm 19.4$  (Swim) vs.  $100 \pm 9.5$  % (Sed);  $p < 0.05$ ).

In isolated cardiomyocytes 24 hours IGF-1 increased cell area ( $114 \pm 1.3$  %;  $p < 0.05$ ) and protein/DNA content ( $115 \pm 3.9$  %,  $p < 0.05$ ), effects not abolished by NHE-1 inhibition with cariporide ( $114 \pm 3$  and  $117 \pm 4.4$  %, respectively). IGF-1 significantly decreased NHE-1 activity during  $\text{pH}_i$  recovery from sustained intracellular acidosis ( $\text{J}_{\text{H}^+}$  at  $\text{pH}_i$  6.8:  $4.08 \pm 0.74$  and  $9.09 \pm 1.21$  mmol/L/min, IGF-1 vs. control;  $p < 0.05$ ), and abolished myocardial slow force response to stretch; IGF-1R, IGF-1 receptor.

**Conclusions:** NHE-1 hyperactivity seems not to be involved in physiological CH development, contrary to what characterizes pathological CH. We propose that AKT, through an inhibitory phosphorylation of the NHE-1, prevents its stretch-induced activation. This posttranslational modification emerges as an adaptive mechanism that avoids NHE-1 hyperactivity preserving its housekeeping functioning.

© 2014 Elsevier Ltd. All rights reserved.

**Abbreviations:** Sed, sedentary, not-trained rats; Swim, swim-trained rats; CH, cardiac hypertrophy; NHE-1,  $\text{Na}^+/\text{H}^+$  exchanger isoform 1; ERK1/2, extracellular signal-regulated kinase 1 and 2; PI3K, phosphatidylinositol 3-kinase; p90<sup>RSK</sup>, 90 kDa ribosomal S6 protein kinase; AKT, protein kinase-B; IGF-1, insulin-like growth factor-1; SFR, slow force response to stretch; IGF-1R, IGF-1 receptor.

\* Corresponding author at: Centro de Investigaciones Cardiovasculares, Facultad de Ciencias Médicas, UNLP, Calle 60 y 120, 1900, La Plata, Argentina. Tel./fax: +54 221 483 4833.

E-mail address: [iennis@med.unlp.edu.ar](mailto:iennis@med.unlp.edu.ar) (I.L. Ennis).

## 1. Introduction

Chronic hemodynamic overload induces the development of cardiac hypertrophy (CH) defined as an increase in heart mass primarily due to the enlargement of individual myocytes. It can be distinguished between physiological CH, an adaptive response of the heart to the increase in workload induced by exercise training or pregnancy, and pathological CH that occurs in the setting of cardiovascular pathologies such as hypertension or cardiac infarction and represents an independent risk factor for cardiovascular morbidity and mortality. It is associated with cardiac fibrosis, loss of cardiac myocytes, re-expression of the

fetal gene program and, even more importantly, with heart failure development. In contrast, physiological CH is characterized by a reversible mild growth of cardiac mass; typically a 10–20% increase, with preserved myocardial structure and normal or even enhanced cardiac performance [1].

Increased workload is transduced into mechanical stretch in the myocardium triggering the release of several humoral factors such as angiotensin II, endothelin 1 and insulin-like growth factor 1 (IGF-1) [2,3]. Human and animal studies have demonstrated that certain factors are preferentially released depending on the nature of stimuli; i.e. pathological or physiological. IGF-1 is increased during postnatal development as well as in response to exercise training [4,5]. Not only has it been reported that cardiac formation of IGF-1 is increased in athletes compared with healthy sedentary controls [5] but also studies in transgenic mice have confirmed the importance of IGF-1 signaling in physiological CH. A mice model overexpressing the IGF-1 receptor (IGF-1R) in the heart displayed physiological CH and a greater hypertrophic response to swim-training compared to control [6] while mice with cardiomyocyte specific knockdown of the same receptor were resistant to exercise-induced CH [7]. IGF-1 stimulates two canonical pathways in cardiomyocytes: the PI3K/AKT pathway, the main intracellular signaling cascade involved in exercise-induced physiological hypertrophy, and the ERK pathway [8]. Moreover, inhibition of PI3K or genetic ablation of AKT1 prevents physiological CH [6,9,10] while overexpression of a constitutively active p110 $\alpha$  PI3K results in physiological CH [11]. On the other hand, pathological CH mostly involves angiotensin II/endothelin 1 release and activation of Gq protein-coupled receptors.

The cardiac Na<sup>+</sup>/H<sup>+</sup> exchanger (NHE-1), a plasma membrane protein that catalyzes the exchange of intracellular H<sup>+</sup> for extracellular Na<sup>+</sup> plays a key physiological role in the regulation of intracellular pH (pH<sub>i</sub>), Na<sup>+</sup> concentration and cell volume. Importantly, it has also been implicated in pathological CH and chronic heart disease. Hemodynamic overload stretches the myocardium triggering an autocrine/paracrine signaling cascade that activates the ERK/p90<sup>RSK</sup> pathway leading to NHE-1 phosphorylation and hyperactivity [3,12]. As a consequence, intracellular Na<sup>+</sup> content augments favoring the reverse mode of the Na<sup>+</sup>/Ca<sup>2+</sup> exchanger. The resulting increase in intracellular Ca<sup>2+</sup> promotes the activation of the prohypertrophic calcineurin/NFAT pathway, critical for pathological but not physiological CH. Moreover, NHE-1 specific inhibition prevents or induces the regression of pathological CH while its hyperactivity is sufficient to induce pathological CH [3,13]. However, the role of the NHE-1 in physiological CH has not been elucidated yet.

Despite the differences in the intracellular signaling activated; myocardial stretch -induced by hemodynamic overload- seems to be a common triggering stimulus for physiological and pathological CH. Thus, we speculate that NHE-1 hyperactivity could be involved in both types of CH leading to Na<sup>+</sup> and Ca<sup>2+</sup> overload and calcineurin activation. However, as we previously mentioned, calcineurin is not involved in physiologic CH development [14]. We hypothesize that during physiological CH stretch-induced NHE-1 hyperactivity is prevented by an inhibitory AKT-dependent phosphorylation of the exchanger that has already been proposed [15]. This posttranslational modification of the NHE-1 would drive CH development to the physiological pattern instead. To test this hypothesis, both *in vivo* and *in vitro* rat models of physiological hypertrophy were used.

## 2. Material and methods

All procedures followed during this investigation conform to the Guide for the Care and Use of Laboratory Animals published by the US National Institutes of Health (NIH Publication No. 85-23, revised 1996) and the experimental protocol was approved by the Animal Welfare Committee of La Plata School of Medicine.

### 2.1. Animals and swim-training protocol.

Male 4-month-old Wistar rats were kept on a 12:12-h light-dark cycle and fed ad libitum. The rats were randomly assigned to a sedentary (Sed) or swim-trained (Swim) group.

Training sessions were performed during the rats' dark cycle and consisted of twice/day 90-min swimming periods, five days/week during 12 weeks in warmed water (30–32 °C). Exercise duration was increased gradually until rats swim during 90 min. Rats in the Sed group were placed in the swimming apparatus for 10 min twice a week to mimic the water stress associated with the experimental protocol. This swimming protocol has been characterized by Medeiros et al. [16] as low to moderate intensity and long duration due to improvement in muscle oxidative capacity.

At the end of the experimental protocol, rats (body weight 300–400 g) were anaesthetized by intraperitoneal injection of sodium pentobarbital (35 mg/kg body weight) and hearts rapidly excised when plane three of anesthesia was reached. The left ventricle (LV) with the septum were weighed (LVW) and normalized by tibial length (TL) to determine cardiac mass.

### 2.2. Echocardiographic examination

Rats were monitored echocardiographically with an ATL Ultramark 6 equipment under light anaesthesia (isoflurane 2%) by 2-dimensional M-mode echocardiography with a 7-MHz transducer at the beginning and end of the protocol. Measurements were performed according to the American Society of Echocardiography leading-edge method [17]. LV mass index (LVMI); relative wall thickness (RWT); LV end-diastolic dimension (LVDD); LV end systolic dimension (LVSD) and end systolic stress were calculated as previously described [18]. Global LV systolic function was assessed by calculating ejection fraction [LVEF: (LVDD<sup>3</sup> – LVSD<sup>3</sup>) × 100/LVDD<sup>3</sup>] and the corrected endocardial fractional shortening (ES) that was expressed as the percentage of the predicted value according to the calculating end systolic stress. Predicted ES were obtained through the correlation between systolic stress and ES previously described reported for Wistar rats [19].

### 2.3. Morphological studies

Ventricular tissue was fixed in buffered 10% formaldehyde and paraffin-embedded. LV coronal sections (4  $\mu$ m thick) at the equator were stained with hematoxylin-eosin or picosirius red (Direct Red 80 Aldrich) for blinded determination of cardiomyocyte cross-sectional area (CSA) and quantitation of collagen volume fraction (CVF) respectively [20,21]. The investigator was unaware of the treatment groups and codes were disclosed after statistical analyses.

### 2.4. Real time RT-PCR

Brain natriuretic peptide (BNP) mRNA expression was assessed by real-time RT-PCR and normalized to GAPDH following the procedure described previously [22].

### 2.5. Western blotting

Left ventricles or isolated cardiac myocytes were homogenized in RIPA buffer (Santa Cruz Biotechnology, sc-24948) with protease inhibitors cocktail, PMSF and sodium orthovanadate. After a brief centrifugation the supernatant was kept and protein concentration determined by the Bradford method (Bio-Rad dye reagent) as described by the manufacturer with BSA as a standard. Samples were denatured and equal amounts of protein were subjected to PAGE and electrotransferred to PVDF membranes. Membranes were then blocked with non-fat-dry milk and incubated overnight with the specific antibodies against: phospho-ERK1/2 (Santa Cruz Biotechnology, sc-16982), phospho-AKT

(Cell Signaling, 4060S), phospho-p90<sup>RSK</sup> (Cell Signaling #9341), phospho-GSK-3 $\beta$  (Cell Signaling #9336), NHE-1 (Santa Cruz Biotechnology sc-28758), calcineurin A $\beta$  (Santa Cruz Biotechnology sc-6124) and PI3 kinase p110 $\alpha$  (Santa Cruz Biotechnology sc-7174). To determine NHE-1 phosphorylation at Ser703 or Ser648, the samples were immunoprecipitated using the NHE-1 polyclonal antibody and then subjected to PAGE, electrotransferred, blocked and incubated with anti-P-14-3-3 binding motif antibody (Cell Signaling, #9601) or anti-P-AKT substrate (Cell Signaling, #10001S) as previously described [15, 23]. IGF-1R phosphorylation was determined in immunoprecipitated samples with IGF-1R $\beta$  antibody (Santa Cruz Biotechnology, sc-81167) and blotted with anti-phosphotyrosine antibody (Santa Cruz Biotechnology, PY20 sc-508) as previously described [24].

For NFAT quantitation cytosolic and nuclear rich fractions were prepared and anti-NFAT antibody (Santa Cruz Biotechnology, sc-8321) was used following a protocol described previously [25].

To normalized the amount of the phosphorylated proteins the membranes were stripped and probed with an antibody that specifically detects total ERK2 (phosphorylated and non-phosphorylated, Santa Cruz Biotechnology, sc-1647), total AKT (Cell signaling, # 9272), total p90<sup>RSK</sup> (Santa Cruz Biotechnology sc-74575), total GSK-3 $\beta$  (Cell Signaling #9315) and NHE-1 (sc-28758). The detection of GAPDH (Millipore MAB374) was used as loading control. Peroxidase-conjugated anti-rabbit (NA934, GE Healthcare Life Sciences), anti-mouse (NA931, GE Healthcare Life Sciences) or anti-goat IgG (sc-2004) were used as secondary antibodies and bands were visualized using the ECL-Plus chemiluminescence detection system (GE Healthcare). Autoradiograms were analyzed by densitometry (Scion Image).

## 2.6. Cell isolation and culture

Rat ventricular myocytes were isolated according to the technique previously described [26]. Briefly, the hearts were attached via the aorta to a cannula, excised, and mounted in a Langendorff apparatus. They were then retrograde perfused at 37 °C with Krebs-Henseleit solution (K-H) of the following composition (in mmol/L): 146.2 NaCl, 4.7 KCl, 1 CaCl<sub>2</sub>, 10 HEPES, 0.35 NaH<sub>2</sub>PO<sub>4</sub>, 1 MgSO<sub>4</sub>, and 10 glucose (pH adjusted to 7.4 with NaOH). The solution was continuously bubbled with 100 % O<sub>2</sub>. After a stabilization period of 4 min, the perfusion was switched to a nominally Ca<sup>2+</sup>-free K-H for 4 min. Hearts were then recirculated with collagenase (115 units/ml) and 1% BSA in K-H containing 60  $\mu$ M CaCl<sub>2</sub>. Perfusion continued until hearts became flaccid (9–11 min). Hearts were then removed from the perfusion apparatus by cutting at the atrioventricular junction. The disaggregated myocytes were separated from the undigested tissue and rinsed several times with a K-H solution containing 1% BSA. The CaCl<sub>2</sub> concentration of K-H solution was increased in four steps to 1 mmol/L. Myocytes were kept in 1 mmol/L CaCl<sub>2</sub> K-H solution at room temperature (20–22 °C) until use.

Isolated cardiac myocytes were attached with laminin and cultured with sodium bicarbonate buffered Medium 199 (M199 Life Technologies), supplemented with (mmol/L): creatine, 5; L-carnitine, 2; taurine, 5 and 100 I.U./ml penicillin and 100  $\mu$ g/ml streptomycin. The treatment was: 1) Control, 2) IGF-1 10 nmol/L, 3) IGF-1 + cariporide (carip, NHE-1 inhibitor, 10  $\mu$ mol/L [27,28]), 4) carip, 5) IGF-1 + AG1024 [IGF-1 receptor (IGF-1R) inhibitor, 100 nmol/L]; 6) AG1024. The inhibitors were added 10 min before IGF-1.

## 2.7. Cell area

Cell area was quantified in a blinded manner in a minimum of 100 cardiomyocytes per experimental condition from at least 3 different rats. After digitalization at 200x magnification in an image analysis system (Image-Pro Plus software), cell area was calculated from the cell perimeter drawn with the mouse and the average was recorded.

## 2.8. Total mass of cellular protein and total content of cellular DNA

We used a technique previously described [29]. Briefly, after 24 hs. of culture the attached cardiomyocytes were thoroughly washed with ice-cold phosphate-buffered saline (pH 7.4), and 10% trichloroacetic acid was added. Cells were kept under these conditions at 4°C for 12 hours to precipitate proteins. Protein concentration was determined by the Bradford method (Bio-Rad dye reagent, Bio-Rad, Hercules, CA, USA) as described by the manufacturer with BSA as a standard. DNA concentration was quantified by fluorometry (Qubit fluorometer, Life Technologies), a quantitation system relying on dyes that only fluoresce when bound to specific molecules, such as dsDNA, ssDNA or RNA. The instrument was calibrated with the Quant-iT dsDNA BR Assay, according to the manufacturer's instructions [30,31]. The ratio of protein to DNA was then calculated to estimate potential protein synthesis [32].

## 2.9. NHE-1 activity

Intracellular pH (pH<sub>i</sub>) was measured in fresh single isolated myocytes superfused with the K-H solution (bicarbonate free) with an epi-fluorescence system (Ion Optix, Milton, MA) following the previously described BCECF epifluorescence technique [33]. The experiments were performed in HCO<sub>3</sub><sup>-</sup> free solution since under this condition the NHE-1 is the only alkalinizing mechanism active. Briefly, myocytes were incubated at room temperature for 10 min with 10  $\mu$ M BCECF-AM (Life Technologies) followed by 30 min washout. Dye-loaded cells were placed in a chamber on the stage of an inverted microscope (Nikon TE 2000-U) and continuously superfused with the K-H solution. Dual excitation (440 and 495 nm) was provided by a 75-watt Xenon arc lamp and transmitted to the myocytes. Emitted fluorescence was collected with a photomultiplier tube equipped with a band-pass filter centred at 535 nm. The 495-to-440 nm fluorescence ratio was digitized at 10 kHz (ION WIZARD fluorescence analysis software). At the end of each experiment, the fluorescence ratio was converted to pH by *in vivo* calibrations using the high K<sup>+</sup>-nigericin method [34].

NHE-1 activity was assessed by evaluating the rate of pH<sub>i</sub> recovery from an ammonium pre-pulse induced acid load [33]. IGF-1 was added 10 minutes before the ammonium pre-pulse (20 mmol/L NH<sub>4</sub>Cl for 2 min) and maintained during the whole experiment. The duration of intracellular acidosis was extended for 2 min by washout of NH<sub>4</sub>Cl with Na<sup>+</sup>-free solution and NHE-1 was reactivated by reintroduction of extracellular Na<sup>+</sup> [33]. Proton efflux (JH) was calculated as dpH<sub>i</sub>/dt  $\times$   $\beta$ <sub>i</sub> and comparison among different groups was done at a common pH<sub>i</sub> of 6.8. The dpH<sub>i</sub>/dt at each pH<sub>i</sub> was obtained from an exponential fit of the recovery phase.  $\beta$ <sub>i</sub> is the intracellular buffering capacity of the myocytes and was measured by exposing cells to varying concentrations of NH<sub>4</sub>Cl in 2 Na<sup>+</sup>-free HEPES bathing solution. pH<sub>i</sub> was allowed to stabilize in Na<sup>+</sup>-free solution before application of NH<sub>4</sub>Cl.  $\beta$ <sub>i</sub> was calculated from the following equation:  $\text{NH}_4^+_{\text{i}} = \text{NH}_4^+_{\text{o}} \times 10^{(\text{pH}_0 - \text{pH}_i)}$  /  $1 + 10^{(\text{pH}_0 - \text{pK})}$  and  $\beta_i = \Delta[\text{NH}_4^+] / \Delta\text{pH}_i$  and referred to the mid-point values of the measured changes in pH<sub>i</sub>.  $\beta_i$  at different pH<sub>i</sub> were estimated from the least squares regression lines  $\beta_i$  vs. pH<sub>i</sub> plots [33]. Where used, the PI3K inhibitor (100 nmol/L wortmannin) and the AKT inhibitor (500 nmol/L MK2206) were added to cells 5 minutes before NH<sub>4</sub>Cl exposure and were present throughout the rest of the protocol. Since both inhibitors were dissolved in DMSO (final concentration 0.01%), the potential effect of this solvent on pH<sub>i</sub> recovery was also evaluated.

## 2.10. Myocardial stiffness and slow force response

Papillary muscles from the left ventricle were used to measure the myocardial stiffness and to assess the slow force response (SFR) to stretch as previously described [35]. Briefly, the muscles were mounted in a perfusion chamber placed on the stage of an inverted microscope (Olympus) and superfused at a constant rate (5 ml/min) with a CO<sub>2</sub>/HCO<sub>3</sub><sup>-</sup>-buffered solution containing (mmol/L): NaCl 128.3, KCl

**Table 1**  
Cardiac morphometric and functional evaluation in sedentary and trained rats.

	Sedentary rats	Swimming-trained rats
BW (g)	476.6 ± 18.9	438.7 ± 7.3
LVW/BW (mg/g)	1.48 ± 0.04	1.67 ± 0.04*
LVW/TL (mg/mm)	22.04 ± 0.26	24.27 ± 0.73*
LVMI (mg/g)	1.5 ± 0.05	1.8 ± 0.02*
LVDD (mmm)	6.68 ± 0.07	7.07 ± 0.05*
LVSD (mm)	2.67 ± 0.06	2.97 ± 0.04*
RWT	0.49 ± 0.01	0.46 ± 0.01*
cFS	96.71 ± 1.15	93.54 ± 1.26
eSS (mm Hg)	128.8 ± 2.85	141.4 ± 3.42*
LVEF (%)	93.6 ± 0.34	92.53 ± 0.43

The values are expressed as mean ± standard error, n = 5 for each group. BW: Body weight, LVW: left ventricular weight, TL: tibial length, LVMI: left ventricular mass index, LVDD: left ventricular diastolic diameter; LVSD: left ventricular systolic diameter; RWT: relative wall thickness, cFS: corrected endocardial fractional shortening, eSS: end systolic stress; LVEF: left ventricular ejection fraction. \* indicates p < 0.05 vs. sedentary rats.

4.5, CaCl<sub>2</sub> 1.35, NaHCO<sub>3</sub> 20.23, MgSO<sub>4</sub> 1.05, glucose 11.0 and equilibrated with 5% CO<sub>2</sub>–95% O<sub>2</sub> (pH ~7.40). The possible participation of catecholamines released by the nerve endings was prevented by adrenergic receptor blockade with 1.0 μmol/L prazosin plus 1.0 μmol/L atenolol. The muscles were paced at 0.2 Hz at a voltage 10% over threshold maintained at 30 °C, and isometric contractions were recorded. Cross sectional area (calculated as 0.75 of the product of thickness and width) was used to normalize force records obtained with a silicon strain gauge (model AEM 801, Sensoron Technologies, Horten, Norway). The slack length of each muscle was determined after mounting, and then the muscles were progressively stretched to the length at which they developed maximal twitch force (L<sub>max</sub>). For myocardial stiffness the length/tension relationship for each muscle was fitted to

an exponential equation. From the fitted curves, fixed values of strains (ΔL/L<sub>max</sub>) were interpolated in each experiment. For SFR measurements the muscles were shortened to obtain the 95% of the maximal twitch force (length that approximated 98% of L<sub>max</sub> and referred to as L<sub>98</sub>). Then, the muscles were shortened to 92% of L<sub>max</sub> (L<sub>92</sub>) and maintained at this length until the beginning of the experimental protocol, when they were abruptly stretched from L<sub>92</sub> to L<sub>98</sub>. IGF-1 was added to the perfusate 20 min before stretch, and during this period, no significant modifications of the developed force were detected.

2.11. Chemicals

All drugs used in the present study were analytical reagent. IGF-1: recombinant mouse insulin like growth factor -1 from Gibco by Life Technologies (Cat # PMG0075); AG1024 (Cat # sc-205907) from Santa Cruz Biotechnology; cariporide: HOE642 from Aventis; AKT inhibitor MK2206 from Selleck Chemicals (Cat # S1078); wortmannin from Sigma, Argentina (Cat # W1628). Wortmannin, MK2206 and AG1024 were diluted in DMSO (final concentration 0.01%). All other drugs were diluted in water.

2.12. Statistics

Results are expressed as mean ± SEM. The Student t test or 1-way ANOVA followed by the Student-Newman-Keuls test were used when corresponding. Significance level was set at p < 0.05.

3. Results

The swimming routine assayed succeeded to induce the development of eccentric CH as revealed by the echocardiographic evaluation

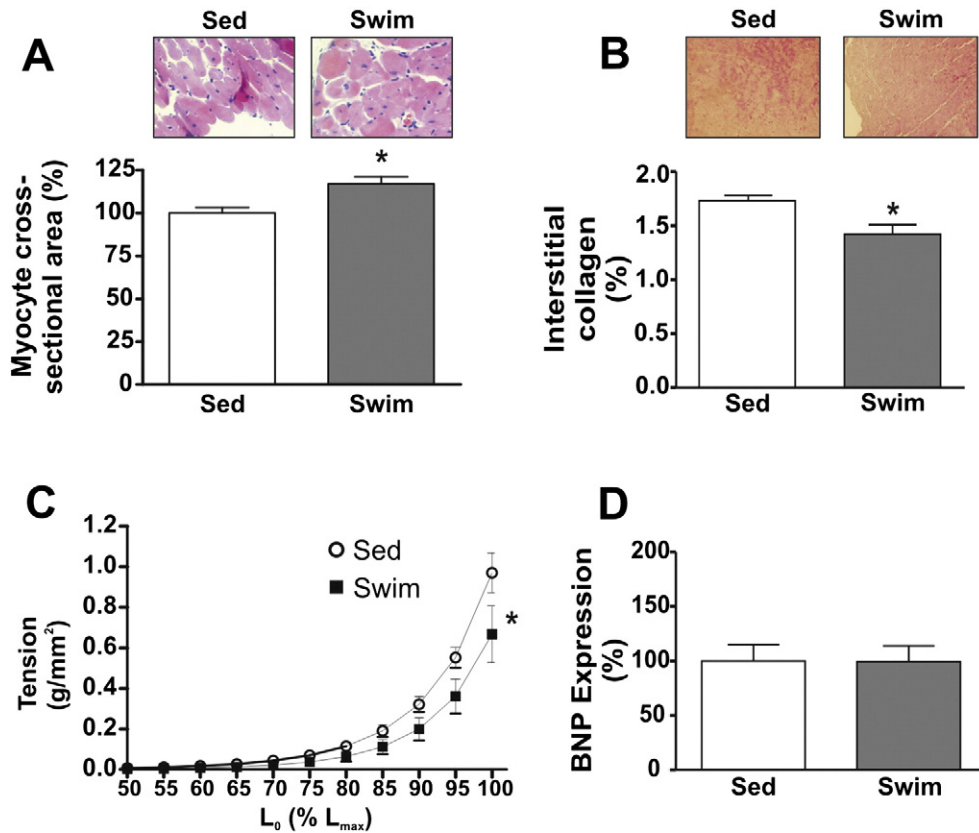


**Fig. 1.** After 12 weeks of swim-training an increase in myocytes cross sectional area (A) and a reduction in myocardial collagen abundance (B) accompanied by decreased myocardial stiffness (C) were detected in the swim-trained rats (Swim) compared to the sedentary ones (Sed). The absence of myocardial fibrosis in the histological examination together with the lack of up-regulation in the expression of BNP -a molecular marker of pathological CH in the trained rats (D) support the physiological nature of the cardiac hypertrophy developed in this experimental model. \* indicates P < 0.05 vs. Sed; n = 5 for each experimental group.

as well as the LVW/BW and LVW/TL ratios. LV systolic function was similar between both experimental groups although a significant increase in end systolic stress was detected in trained rats (Table 1). The increase in cardiomyocyte cross sectional area and the absence of myocardial fibrosis in the histological sections, together with the lack of up-regulation of BNP -a molecular marker of pathological CH- support the physiological nature of the CH developed. The decrease in myocardial collagen content in the Swim group was accompanied by a reduction in myocardial stiffness evaluated by the length/tension relation in papillary muscles (Fig. 1).

As it was expected, the swimming routine induced the activation of the PI3K/AKT and ERK1/2-p90<sup>RSK</sup> signaling pathways in the hypertrophied myocardium (Figs. 2A and B). However, the activity of the calcineurin/NFAT prohypertrophic pathway -explored by assessing the expression of calcineurin A $\beta$  as well as the nuclear abundance of NFAT- was not stimulated supporting that the hypertrophy developed was of the physiological type (Figs. 2C and D). Since we have previously demonstrated that myocardial stretch induces the phosphorylation of the NHE-1 cytosolic regulatory tail at Ser703 by p90<sup>RSK</sup> and this post-translational modification is accompanied by the hyperactivity of the exchanger [12], we examine this parameter in the myocardium of the trained rats. Surprisingly, we were able to detect a significant increase in NHE-1 phosphorylation at this site with no change in the exchanger expression (Figs. 3A and B). However, NHE-1 hyperactivity appears unlikely since calcineurin, critical for pathological but not physiological CH, seems not to be activated as we already mentioned. We also evaluate NHE-1 phosphorylation at Ser648, a recognized target for AKT that has been described to inhibit NHE-1 activity, and found that the exchanger was also significantly phosphorylated at this residue in the hypertrophied myocardium of the trained rats (Fig. 3C), probably opposing at the functional level to the effect of p90<sup>RSK</sup>.

In order to get further insight into the role played by the NHE-1 we set up an *in vitro* model of physiological CH. Adult rat ventricular

myocytes were incubated in the presence of 10 nmol/L IGF-1 and 24 hours later cardiomyocyte growth was evaluated. As it can be appreciated in Figs. 4A-C, IGF-1 induced an increase in cell area and in the protein/DNA ratio – confirming the occurrence of cardiomyocyte hypertrophy – of a similar magnitude to the hypertrophic response detected in the rats subjected to swim-training. Interestingly, co-incubation of IGF-1 with the NHE-1 selective inhibitor cariporide did not prevent the hypertrophic response, suggesting that NHE-1 hyperactivity was not involved in the effect of IGF-1. On the contrary, the specific blockade of the IGF-1R with AG1024 completely blunted cardiomyocyte growth. BNP expression was not up-regulated by IGF-1, supporting the physiological nature of this type of hypertrophy (Fig. 4D). Neither the inhibitors nor the diluent used exerted an effect on cell growth in the absence of IGF-1.

As expected, IGF-1 increased IGF-1R tyrosine phosphorylation, and similarly to the *in vivo* data, it also stimulated AKT and ERK1/2 phosphorylation, actions prevented by AG1024 (Figs. 5A–C). Inhibition of PI3K with wortmannin prevented AKT activation but not ERK phosphorylation, since IGF-1 most likely activates the ERK pathway independently of PI3K and probably through the recruitment of Grb2 protein [8]. IGF-1-induced AKT activation was confirmed by assessing the phosphorylation of one of its critical downstream targets, the kinase GSK-3 $\beta$ . IGF-1 significantly increased phospho-GSK-3 $\beta$ , effect that was prevented by AG1024 (Fig. 5D). We did not detect any effect of 0.01% DMSO (diluent for AG1024 and wortmannin) on these kinases phosphorylation (data not shown). The effect of IGF-1 upon the calcineurin/NFAT pathway was also explored. IGF-1 did not increase either calcineurin A $\beta$  expression or NFAT nuclear translocation, supporting that this pathway was not stimulated in this experimental model of physiological CH (Figs. 5E-F).

Next, we evaluated NHE-1 activity during the recovery from sustained intracellular acidosis. Under this condition, NHE-1 activity is increased not only because of the allosteric stimulation of the exchanger

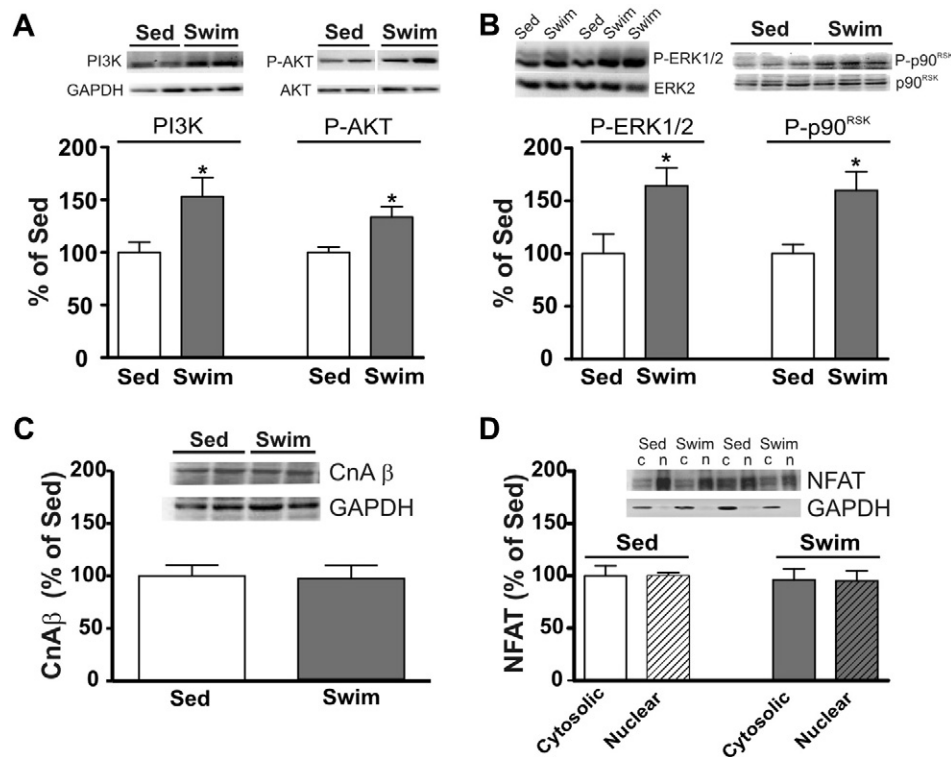


**Fig. 2.** Exercise training induced the activation of the prohypertrophic intracellular signaling pathways mediated by PI3K-AKT (A) and ERK1/2-p90<sup>RSK</sup> (B) whereas CnA $\beta$  expression (C) and NFAT nuclear abundance (D) were not modified in the hypertrophied myocardium supporting the physiological nature of the swimming-induced hypertrophy. Average data are depicted in the bar graphs, and representative blots are shown on top of the bars for each panel figure. Sed and Swim, sedentary and swim-trained rats respectively; "n": nuclear and "c": cytosolic enriched fractions, respectively. GAPDH was used to confirm the efficacy of the fractionation protocol. \* indicates  $P < 0.05$  vs. Sed;  $n = 5$  for each experimental group.

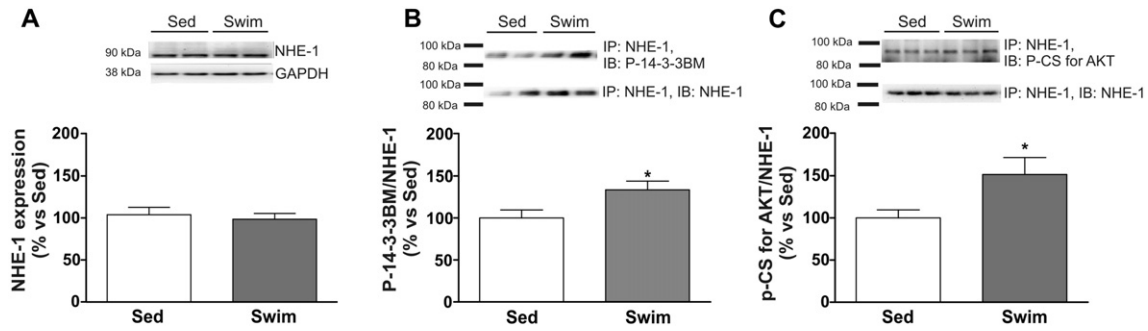


**Fig. 3.** NHE-1 myocardial expression assessed by Western blot was not modified by training (A). We next examined posttranslational modifications of the regulatory domain of the exchanger. A significant increase in the phosphorylation of the recognized target for ERK1/2-p90<sup>RSK</sup>, Ser703, estimated by a specific antibody against P-14-3-3 binding motif (BM), was detected in the hypertrophied myocardium of the trained rats compared to the sedentary ones (B). However, it was also detected an increase in the phosphorylation of the inhibitory consensus site for AKT (CS) in the hypertrophied myocardium of trained rats (C). We hypothesize that the AKT-dependent phosphorylation of the exchanger counterbalances the stimulatory effect of Ser703 phosphorylation. Average data are depicted in the bar graphs and representative blots are shown on top of the bars for each panel figure. Sed and Swim, sedentary and trained rats respectively. \* indicates  $P < 0.05$  vs. Sed;  $n = 5$  for each experimental group.

by intracellular H<sup>+</sup>, but also because of ERK/p90<sup>RSK</sup>-dependent phosphorylation of its cytosolic tail [33,36,37]. IGF-1 significantly decreased NHE-1 activity during intracellular pH recovery and this effect was dependent on PI3K/AKT since it was prevented by the inhibition of this kinase pathway with wortmannin or MK2206 (Fig. 6A). Interestingly, when NHE-1 activity was assessed during the recovery from acute intracellular acidosis, condition in which the exchanger activity seems to exclusively depend on H<sup>+</sup> allosteric stimulation, IGF-1 did not exert any effect (Fig. 6B).

In order to confirm the inhibitory action of IGF-1 upon NHE-1 activity, a new set of experiments was performed in which the effect of IGF-1 on the slow force response to stretch (SFR) was evaluated. The SFR is the slow increase in force that follows the Frank-Starling mechanism in response to myocardial stretch. The underlying mechanism of the SFR is an increase in intracellular Ca<sup>2+</sup> concentration. This occurs through the reverse mode of the Na<sup>+</sup>/Ca<sup>2+</sup> exchanger as a consequence of the increase in intracellular Na<sup>+</sup> caused by the stretch-induced NHE-1 hyperactivity [38]. Isolated rat papillary muscles were subjected to stretch in the absence and presence of IGF-1. The stretching of the papillary muscles in the control group promoted the characteristic biphasic mechanical response; an initial abrupt force increase followed by the SFR (Figs. 7A and D). Next, we confirmed that the SFR depended on NHE-1

activation since it was not present when myocardial stretch was performed in the presence of cariporide (Figs. 6B and D). Interestingly, the SFR was also absent in the papillary muscles pre-incubated with IGF-1 supporting that IGF-1 signaling blunted stretch-induced NHE-1 stimulation (Figs. 7C and D).

**4. Discussion**

We believe the main contribution of this study is the finding that NHE-1 hyperactivity, critical for pathological CH, would not be involved in the development of physiological CH.

After birth, the heart typically enlarges its size primarily through hypertrophy of the individual myocytes, process known as the normal postnatal growth. In addition, the heart may increase its mass in response to hemodynamic overload decreasing wall tension to maintain or even improve cardiac performance, according to Laplace's law. Therefore, although at first glance an increase in cardiac mass may sound beneficial, it is not always the case. While physiological CH is an adaptive reaction of the heart to the increase in workload preserving cardiac performance, pathological hypertrophy increases morbidity and mortality usually evolving to heart failure [39]. Cardiovascular disease continues to be not only the leading cause of death in the developed world but

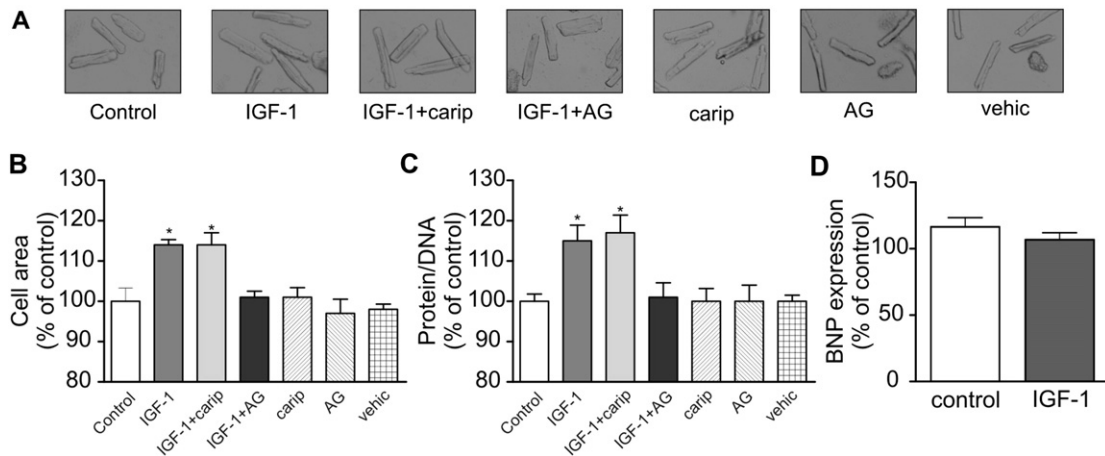


**Fig. 4.** Isolated rat ventricular myocytes were cultured in the presence of 10 nmol/L IGF-1 during 24 hours. Representative micrographs from each experimental group are shown in panel A. IGF-1 induced a significant increase in cell area (B, values represent the mean ± standard error of a minimum 100 cardiomyocytes per experimental condition) and in the protein/DNA ratio (C), confirming cardiomyocyte hypertrophy. The hypertrophy induced was of a similar magnitude to the detected in the swim-trained rats (~14%). Interestingly, NHE-1 selective inhibition with 10 μmol/L cariporide (carip) did not prevent cardiomyocyte growth, suggesting that NHE-1 hyperactivity was not involved in the hypertrophic effect of IGF-1. On the contrary, the specific blockade of the IGF-1 receptor with AG1024 completely blunted IGF-1 effect. (D) In agreement with the result obtained in trained rats, no up-regulation of BNP was detected under IGF-1 stimulation. Neither the inhibitors nor the diluent (DMSO 0.01%) exerted any effect on cell growth in the absence of IGF-1. \* indicates  $P < 0.05$  vs. control.

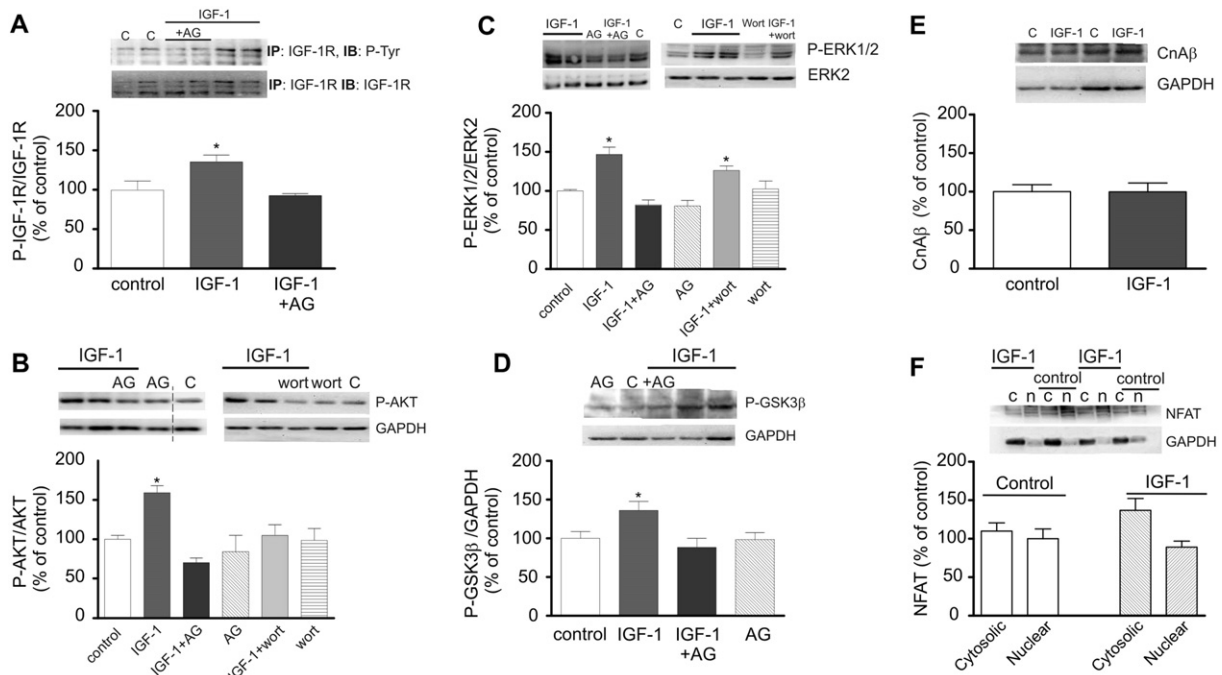


**Fig. 5.** IGF-1 stimulated tyrosine phosphorylation of the IGF-1R and this was blunted by AG1024 (A). Moreover, and similarly to the *in vivo* data, IGF-1 stimulated AKT and ERK1/2 phosphorylation, both actions again prevented by AG1024 (B-C). Inhibition of PI3K with wortmannin prevented AKT activation but not ERK phosphorylation, since IGF-1 most likely activates the ERK pathway independently of PI3K. IGF-1-induced AKT activation was confirmed by assessing the phosphorylation of one of its critical downstream targets, the kinase GSK-3 $\beta$ . IGF-1 significantly increased phospho-GSK-3 $\beta$ , effect that was prevented by AG1024 (D). No effect of IGF-1 was detected upon calcineurin/NFAT prohypertrophic signaling cascade. IGF-1 did not increase calcineurin A $\beta$  expression or NFAT nuclear translocation, supporting that this pathway was not stimulated in the experimental model of physiological CH developed (E-F). "n": nuclear and "c": cytosolic enriched fractions, respectively. GAPDH was used to confirm the efficacy of the fractionation protocol. Average data are depicted in the bar graphs and representative blots are shown on top of the bars. The vertical line in the representative blot shown on the left side of panel B indicates that this blot was spliced (between lanes 4 and 5) in order to show only representative bands from the experimental conditions analyzed. Data are expressed as mean  $\pm$  standard error of at least 4 different experiments per group. \* indicates  $P < 0.05$  vs. control.

also one of the main causes of enormous health cost and worsening of life quality. Therefore elucidating the intracellular signaling pathway underlying the development of physiological CH may provide a blueprint for clinical translation, potentially contributing to the design of novel therapeutic strategies to favor this type of cardiac mass enlargement

in subjects with pathological hemodynamic overload. Moreover, it has been recently reported that swimming-induced physiological CH initiates activation of cardiac progenitor cells [40]. This allows us to speculate not only on the beneficial impact of stimulating physiological cardiomyocyte growth but also the putative opportunity to favor myocardial

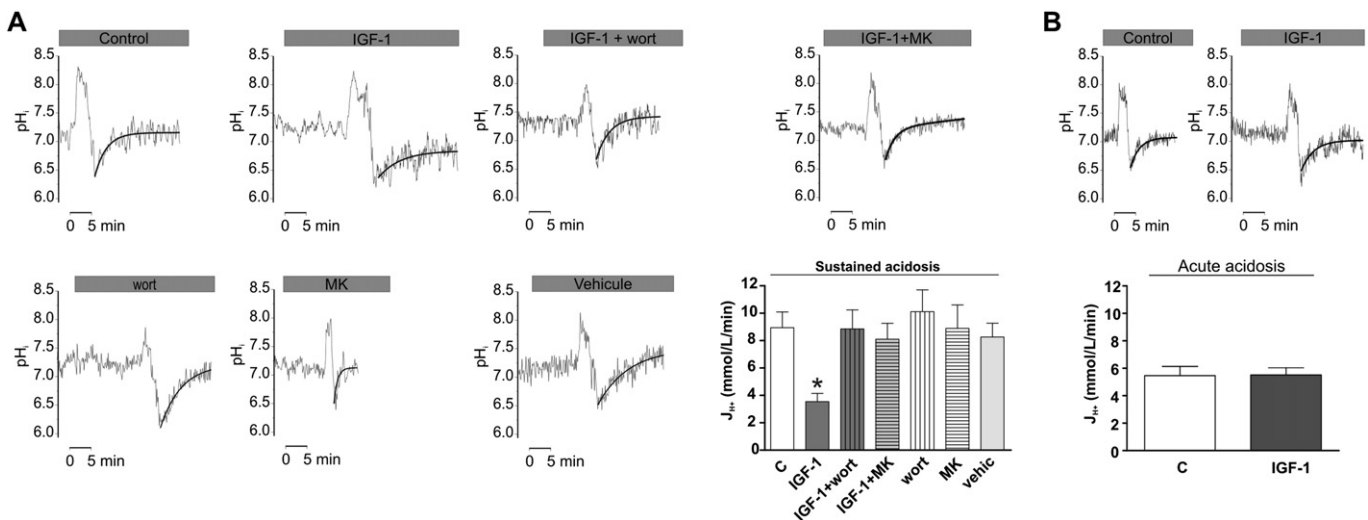


**Fig. 6.** (A) NHE-1 activity was assessed in isolated adult rat ventricular myocytes during the recovery from sustained intracellular acidosis in bicarbonate free medium in order to exclude the involvement of any other intracellular pH regulatory mechanism. During sustained intracellular acidosis NHE-1 activity is increased not only because of the allosteric stimulation by intracellular  $H^+$ , but also because of ERK/p90<sup>RSK</sup>-dependent phosphorylation of the cytosolic tail [33,36,37]. IGF-1 significantly decreased NHE-1 activity during intracellular pH recovery from sustained intracellular acidosis. This effect was mediated by the PI3K/AKT pathway since it was prevented by inhibition of PI3K with 100 nmol/L wortmannin (wort) and by the AKT inhibitor MK2206 (500 nmol/L, MK). Neither the inhibitors nor the diluent (DMSO 0.01%) affected pH recovery in the absence of IGF-1. \* indicates  $P < 0.05$  vs. control. (B) NHE-1 activity was also evaluated during the recovery from acute intracellular acidosis, condition in which the exchanger activity seems to exclusively depend on  $H^+$  allosteric stimulation. IGF-1 did not exert any effect under this experimental condition. NHE-1 activity was measured as proton efflux ( $J_{H^+}$ ) and comparison among the different groups was done at a common intracellular pH of 6.8, as explained in Methods. Data are expressed as mean  $\pm$  standard error of at least 7 cells per experimental group. C = control. \* indicates  $P < 0.05$  vs. control.

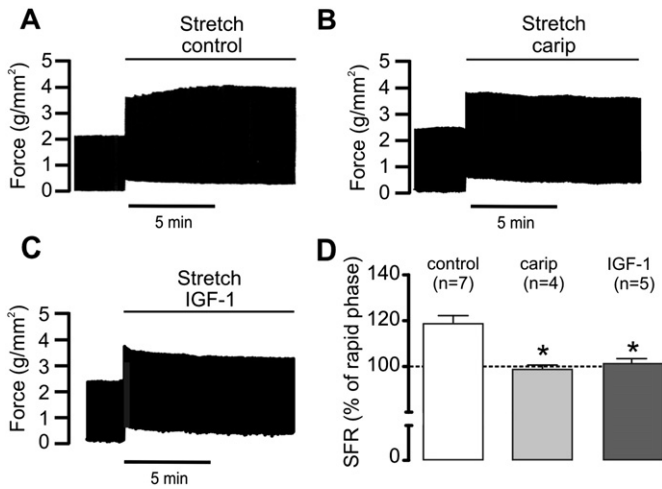


**Fig. 7.** In order to confirm the effect of IGF-1 upon NHE-1 activity, the slow force response (SFR) to stretch was evaluated in isolated rat papillary muscles in the absence and presence of IGF-1. The SFR is the slow increase in force that follows the Frank-Starling mechanism in response to myocardial stretch and depends on the increase in intracellular  $Ca^{2+}$  through the reverse mode of the  $Na^+/Ca^{2+}$  exchanger as a consequence of the increase in intracellular  $Na^+$  due to stretch-induced NHE-1 hyperactivity [38]. The stretching of the papillary muscles in the control group promoted the characteristic biphasic mechanical response; an initial abrupt force increase followed by the SFR (A). On the contrary, the SFR was absent in the papillary muscles pre-incubated with the NHE-1 inhibitor cariporide, confirming the crucial role of this exchanger in the inotropic response to stretch (B). Interestingly, the SFR was also absent in the papillary muscles pre-incubated with IGF-1, supporting that IGF-1 signaling blunted stretch-induced NHE-1 stimulation (C and D). A–C are original force records and D the average results. Carip: cariporide; \* indicates  $P < 0.05$  vs. control.

regeneration by exercise training in pathologies characterized by cardiac tissue loss.

NHE-1 up-regulation has been extensively described as a central component of cardiac pathologies [41]. In line with these findings, NHE-1 inhibition has been repeatedly reported to exert a highly beneficial effect in a variety of diseased animal models [42]. Moreover, it has been demonstrated that NHE-1 hyperactivity is enough to induce pathological CH [13]. On the other hand, the importance of NHE-1 in physiological CH has not been elucidated yet. In this context, we have reported in adult spontaneously hypertensive rats (SHR), in which NHE-1 hyperactivity is critically involved in the development of CH, that endurance training succeed to transform the pathological CH into the physiological type, at the time that calcineurin activity was normalized [21]. The conversion was not only evident at cardiac structure but

also at cardiac performance, evidencing a slight but significant improvement in left ventricular systolic function. Interestingly, we have also demonstrated in the SHR model that NHE-1 inhibition induces the regression of CH and normalization of the calcineurin/NFAT pathway activity, even without normalizing high blood pressure [25]. These data support the antagonism of NHE-1 in the development of pathological CH. NHE-1 hyperactivity increases intracellular  $Na^+$  content favoring the reverse mode of operation of the  $Na^+/Ca^{2+}$  exchanger leading to an increase in intracellular calcium that facilitates calcineurin/NFAT activation. In the present work we did not detected activation of the calcineurin/NFAT pathway in the hypertrophied myocardium of the swim-trained rats, supporting not only the physiological nature of CH but also the absence of NHE-1 hyperactivity in this model.

Regarding to the NHE-1 and exercise training there is very limited data. It has been recently reported that chronic exercising reduces NHE-1 content in the hypertrophied myocardium of female rats [43]. However, in this work it was not assessed NHE-1 activity. On the contrary, moderate to high intensity exercise protocols were reported to increase NHE-1 expression in skeletal muscles enhancing their ability to tolerate acid loads [44,45]. However, contrary to skeletal muscle, the heart is not expected to experience an acid load during exercise [43]. In the present work we explore NHE-1 expression and activity under stimulus for physiological CH. We not only found that NHE-1 was not hyperactive or up-regulated in the physiologically hypertrophied myocardium but also we presented data supporting that IGF-1, the main mediator of physiological hypertrophy, exerts an inhibitory effect upon the exchanger activity. By this mechanism it is possibly prevented intracellular  $Na^+$  and  $Ca^{2+}$  accumulation and calcineurin activation. It is interesting to analyze that even though exercise training exposes the heart to hemodynamic overload and therefore myocardial stretch (a well-recognized stimulus for NHE-1 activation) hyperactivity of the exchanger appears to be prevented in the setup of physiological CH. Based in the present results as well as in previous data [15] we propose that an inhibitory phosphorylation of the NHE-1 triggered by the PI3K/AKT pathway is responsible for this effect. The phosphorylation of the cytosolic tail of the exchanger in a consensus site for AKT, namely Ser648, was previously reported to inhibit the exchanger activity [15]. This posttranslational modification would counterbalance the stimulatory effect mediated by the stretch-activated ERK/p90<sup>RSK</sup> pathway. NHE-1 hyperactivity, as we have already mentioned, plays a key role in pathological CH development by allowing calcium dependent calcineurin/NFAT activation. Dephosphorylated NFAT translocates to the nucleus and triggers the transcription of those genes characteristic of the pathological pattern of CH, finally driving to myocardial hypertrophy and fibrosis. Calcineurin has been repeatedly demonstrated to play

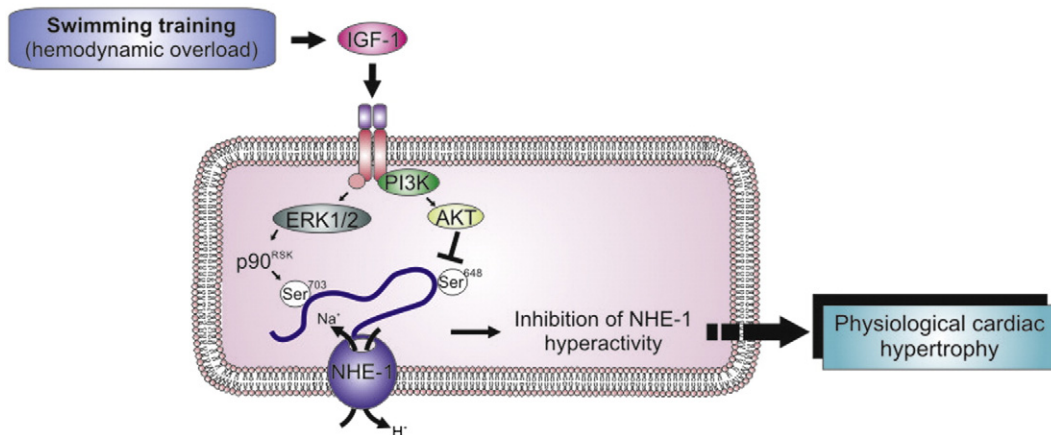


**Fig. 8.** Schematic representation based in our present results as well as in previous data that summarizes our proposal. An inhibitory phosphorylation of the NHE-1 triggered by the PI3K/AKT pathway at Ser648 would counterbalance the stimulatory effect mediated by the ERK/p90<sup>RSK</sup> pathway under conditions of hemodynamic overload. By this mechanism, NHE-1 hyperactivity, critical for pathological cardiac hypertrophy (CH) development does not occur in the setup of physiological CH. Therefore, the inhibitory phosphorylation of the NHE-1 by AKT would be a critical step orienting the intracellular signaling to the development of the physiological but not pathological geno- and phenotype of CH.



a main role in pathological CH but not to be involved in the physiological one [14]. Therefore, the inhibitory phosphorylation of the NHE-1 by AKT would be a critical step orienting the intracellular signaling to the development of the physiological but not pathological geno- and phenotype of CH. Fig. 8 schematically summarizes our proposal.

For the *in vitro* model of physiological CH we chose IGF-1 stimulation of isolated adult cardiomyocytes. It has been demonstrated that IGF-1 expression not only increases in the rat heart in response to swim-training but also in regularly trained athletes [4,5]. Even more important, it has been recently confirmed that IGF-1R signaling is required for exercise-induced cardiac hypertrophy in a mice model with cardiomyocyte-specific knockout of IGF-1R [7]. In this model the knockout mice did not develop CH in response to 5-weeks of swim-training, while the wild type did. Interestingly, Ikeda et al. working with this same transgenic mouse model found that both IGF-1R and the insulin receptor were activated by IGF-1 and exercise, having overlapping or redundant functions in the process of physiological CH [24]. However, under normal conditions IGF-1 signals primarily through its cognate receptor.

In the IGF-1 stimulated cardiomyocytes we were able to induce the hypertrophic response, evidenced by the increase in cell area and the protein/DNA ratio. More notably, a PI3K/AKT-mediated inhibitory effect of IGF-1 upon the NHE-1 was detected preventing NHE-1 hyperactivity during sustained intracellular acidosis. This data was confirmed in the SFR experiments in which the papillary muscles stretched under the presence of IGF-1 did not develop the SFR, the mechanical counterpart of stretch-induced NHE-1 activation.

## 5. Conclusions

Hemodynamic overload induces myocardial stretch and CH development. NHE-1 hyperactivity has been widely reported to be critical for pathological CH development [3]. However, in the context of physiological CH an AKT-dependent inhibitory phosphorylation of the NHE-1 appears to be preventing the exchanger hyperactivity. This posttranslational modification of the NHE-1 emerges as a critical step orienting the intracellular signaling to the development of the physiological but not pathological geno- and phenotype of CH, possibly by preventing intracellular  $\text{Na}^+/\text{Ca}^{2+}$  accumulation and calcineurin/NFAT activation. Importantly, the inhibitory AKT-dependent mechanism describes herein avoids NHE-1 hyperactivity preserving its housekeeping functioning.

## Founding sources

This work was supported in part by grant PICT 2012- 2907 from Agencia Nacional de Promoción Científica de Argentina and M11/165 from Universidad Nacional de La Plata to Dr. Irene L. Ennis.

## Disclosures

None declared.

## Acknowledgements

We specially thank Oscar Andres Pinilla for technical assistance.

## References

- Maillet M, van Berlo JH, Molkenkin JD. Molecular basis of physiological heart growth: fundamental concepts and new players. *Nat Rev Mol Cell Biol* 2013;14:38–48.
- Bernardo BC, Weeks KL, Pretorius L, McMullen JR. Molecular distinction between physiological and pathological cardiac hypertrophy: experimental findings and therapeutic strategies. *Pharmacol Ther* 2010;128:191–227.
- Cingolani HE, Ennis IL. Sodium-hydrogen exchanger, cardiac overload, and myocardial hypertrophy. *Circulation* 2007;115:1090–100.
- Scheinowitz M, Kessler-Icekson G, Freimann S, Zimmermann R, Schaper W, Golomb E, et al. Short- and long-term swimming exercise training increases myocardial insulin-like growth factor-1 gene expression. *Growth Horm IGF Res* 2003;13:19–25.
- Neri Serneri GG, Boddì M, Modesti PA, Cecioni I, Coppo M, Padeletti L, et al. Increased cardiac sympathetic activity and insulin-like growth factor-1 formation are associated with physiological hypertrophy in athletes. *Circ Res* 2001;89:977–82.
- McMullen JR, Shioi T, Huang WY, Zhang L, Tarnavski O, Bisping E, et al. The insulin-like growth factor 1 receptor induces physiological heart growth via the phosphoinositide 3-kinase(p110alpha) pathway. *J Biol Chem* 2004;279:4782–93.
- Kim J, Wende AR, Sena S, Theobald HA, Soto J, Sloan C, et al. Insulin-like growth factor 1 receptor signaling is required for exercise-induced cardiac hypertrophy. *Mol Endocrinol* 2008;22:2531–43.
- Troncoso R, Ibarra C, Vicencio JM, Jaimovich E, Lavandero S. New insights into IGF-1 signaling in the heart. *Trends Endocrinol Metab* 2014;25:128–37.
- DeBosch B, Treskov I, Lupu TS, Weinheimer C, Kovacs A, Courtois M, et al. Akt1 is required for physiological cardiac growth. *Circulation* 2006;113:2097–104.
- McMullen JR, Shioi T, Zhang L, Tarnavski O, Sherwood MC, Kang PM, et al. Phosphoinositide 3-kinase(p110alpha) plays a critical role for the induction of physiological, but not pathological, cardiac hypertrophy. *Proc Natl Acad Sci U S A* 2003;100:12355–60.
- Shioi T, Kang PM, Douglas PS, Hampe J, Yballe CM, Lawitts J, et al. The conserved phosphoinositide 3-kinase pathway determines heart size in mice. *EMBO J* 2000;19:2537–48.
- Cingolani HE, Ennis IL, Aiello EA, Perez NG. Role of autocrine/paracrine mechanisms in response to myocardial strain. *Pflügers Arch* 2011;462:29–38.
- Nakamura TY, Iwata Y, Arai Y, Komamura K, Wakabayashi S. Activation of  $\text{Na}^+/\text{H}^+$  exchanger 1 is sufficient to generate  $\text{Ca}^{2+}$  signals that induce cardiac hypertrophy and heart failure. *Circ Res* 2008;103:891–9.
- Wilkins BJ, Dai YS, Bueno OF, Parsons SA, Xu J, Plank DM, et al. Calcineurin/NFAT coupling participates in pathological, but not physiological, cardiac hypertrophy. *Circ Res* 2004;94:110–8.
- Snabaitis AK, Cuello F, Avkiran M. Protein kinase B/Akt phosphorylates and inhibits the cardiac  $\text{Na}^+/\text{H}^+$  exchanger NHE1. *Circ Res* 2008;103:881–90.
- Medeiros AGR, Kalil LMP, Bacurau RFP, Rosa LFBC, Negrao CE, Brum PC. Efeito do treinamento físico de natacao sobre o sistema cardiovascular de ratos normotensos. *Rev Paul Educacao Fis* 2000;14:7–15.
- Lang RM, Bierig M, Devereux RB, Flachskampf FA, Foster E, Pellikka PA, et al. Recommendations for chamber quantification: a report from the American Society of Echocardiography's Guidelines and Standards Committee and the Chamber Quantification Writing Group, developed in conjunction with the European Association of Echocardiography, a branch of the European Society of Cardiology. *J Am Soc Echocardiogr* 2005;18:1440–63.
- Escudero EM, Camilion de Hurtado MC, Perez NG, Tufare AL. Echocardiographic assessment of left ventricular midwall mechanics in spontaneously hypertensive rats. *Eur J Echocardiogr* 2004;5:169–75.
- de Simone G, Devereux RB, Roman MJ, Ganau A, Saba PS, Alderman MH, et al. Assessment of left ventricular function by the midwall fractional shortening/end-systolic stress relation in human hypertension. *J Am Coll Cardiol* 1994;23:1444–51.
- Camilion de Hurtado MC, Portiansky EL, Perez NG, Rebollo OR, Cingolani HE. Regression of cardiomyocyte hypertrophy in SHR following chronic inhibition of the  $\text{Na}^+/\text{H}^+$  exchanger. *Cardiovasc Res* 2002;53:862–8.
- Garciaarena CD, Pinilla OA, Nolly MB, Laguens RP, Escudero EM, Cingolani HE, et al. Endurance training in the spontaneously hypertensive rat: conversion of pathological into physiological cardiac hypertrophy. *Hypertension* 2009;53:708–14.
- Ennis IL, Garciaarena CD, Perez NG, Dulce RA, Camilion de Hurtado MC, Cingolani HE. Endothelin isoforms and the response to myocardial stretch. *Am J Physiol Heart Circ Physiol* 2005;288:H2925–30.
- Garciaarena CD, Caldiz CI, Portiansky EL, Chiappe de Cingolani GE, Ennis IL. Chronic NHE-1 blockade induces an antiapoptotic effect in the hypertrophied heart. *J Appl Physiol* 2009;106:1325–31.
- Ikeda H, Shiojima I, Ozasa Y, Yoshida M, Holzenberger M, Kahn CR, et al. Interaction of myocardial insulin receptor and IGF receptor signaling in exercise-induced cardiac hypertrophy. *J Mol Cell Cardiol* 2009;47:664–75.
- Ennis IL, Garciaarena CD, Escudero EM, Perez NG, Dulce RA, Camilion de Hurtado MC, et al. Normalization of the calcineurin pathway underlies the regression of hypertensive hypertrophy induced by  $\text{Na}^+/\text{H}^+$  exchanger-1 (NHE-1) inhibition. *Can J Physiol Pharmacol* 2007;85:301–10.
- Aiello EA, Cingolani HE. Angiotensin II stimulates cardiac L-type  $\text{Ca}^{2+}$  current by a  $\text{Ca}^{2+}$ - and protein kinase C-dependent mechanism. *Am J Physiol Heart Circ Physiol* 2001;280:H1528–36.
- De Giusti VC, Garciaarena CD, Aiello EA. Role of reactive oxygen species (ROS) in angiotensin II-induced stimulation of the cardiac  $\text{Na}^+/\text{HCO}_3^-$  cotransport. *J Mol Cell Cardiol* 2009;47:716–22.
- van Borren MM, Baartscheer A, Wilders R, Ravesloot JH. NHE-1 and NBC during pseudo-ischemia/reperfusion in rabbit ventricular myocytes. *J Mol Cell Cardiol* 2004;37:567–77.
- Correa MV, Nolly MB, Caldiz CI, de Cingolani GE, Cingolani HE, Ennis IL. Endogenous endothelin 1 mediates angiotensin II-induced hypertrophy in electrically paced cardiac myocytes through EGFR transactivation. *Pflügers Arch* 2014;466(9):1819–30. <http://dx.doi.org/10.1007/s00424-013-1413-y>.
- Simbolo M, Gottardi M, Corbo V, Fassan M, Mafficini A, Malpeli G, et al. DNA qualification workflow for next generation sequencing of histopathological samples. *PLoS One* 2013;8:e62692.
- Li Z, Huang J, Zhao J, Chen C, Wang H, Ding H, et al. Rapid molecular genetic diagnosis of hypertrophic cardiomyopathy by semiconductor sequencing. *J Transl Med* 2014;12:173.

- [32] Gruson D, Ginion A, Decroly N, Lause P, Vanoverschelde JL, Ketelslegers JM, et al. Urotensin II induction of adult cardiomyocytes hypertrophy involves the Akt/GSK-3 $\beta$  signaling pathway. *Peptides* 2010;31:1326–33.
- [33] Yeves AM, Garcarena CD, Nolly MB, Chiappe de Cingolani GE, Cingolani HE, Ennis IL. Decreased activity of the Na<sup>+</sup>/H<sup>+</sup> exchanger by phosphodiesterase 5A inhibition is attributed to an increase in protein phosphatase activity. *Hypertension* 2010;56:690–5.
- [34] Perez NG, Alvarez BV, Camilion de Hurtado MC, Cingolani HE. pH<sub>i</sub> regulation in myocardium of the spontaneously hypertensive rat. Compensated enhanced activity of the Na<sup>+</sup>-H<sup>+</sup> exchanger. *Circ Res* 1995;77:1192–200.
- [35] Perez NG, de Hurtado MC, Cingolani HE. Reverse mode of the Na<sup>+</sup>-Ca<sup>2+</sup> exchange after myocardial stretch: underlying mechanism of the slow force response. *Circ Res* 2001;88:376–82.
- [36] Haworth RS, McCann C, Snabaitis AK, Roberts NA, Avkiran M. Stimulation of the plasma membrane Na<sup>+</sup>/H<sup>+</sup> exchanger NHE1 by sustained intracellular acidosis. Evidence for a novel mechanism mediated by the ERK pathway. *J Biol Chem* 2003;278:31676–84.
- [37] Haworth RS, Dashnyam S, Avkiran M. Ras triggers acidosis-induced activation of the extracellular-signal-regulated kinase pathway in cardiac myocytes. *Biochem J* 2006;399:493–501.
- [38] Cingolani HE, Perez NG, Cingolani OH, Ennis IL. The Anrep effect: 100 years later. *Am J Physiol Heart Circ Physiol* 2013;304:H175–82.
- [39] Levy D, Garrison RJ, Savage DD, Kannel WB, Castelli WP. Prognostic implications of echocardiographically determined left ventricular mass in the Framingham Heart Study. *N Engl J Med* 1990;322:1561–6.
- [40] Xiao J, Xu T, Li J, Lv D, Chen P, Zhou Q, et al. Exercise-induced physiological hypertrophy initiates activation of cardiac progenitor cells. *Int J Clin Exp Pathol* 2014;7:663–9.
- [41] Wakabayashi S, Hisamitsu T, Nakamura TY. Regulation of the cardiac Na<sup>+</sup>/H<sup>+</sup> exchanger in health and disease. *J Mol Cell Cardiol* 2013;61:68–76.
- [42] Karmazyn M. NHE-1: still a viable therapeutic target. *J Mol Cell Cardiol* 2013;61:77–82.
- [43] Feger BJ, Starnes JW. Myocardial Na<sup>+</sup>/H<sup>+</sup> exchanger-1 (NHE1) content is decreased by exercise training. *J Physiol Biochem* 2013;69:8.
- [44] Iaia FM, Thomassen M, Kolding H, Gunnarsson T, Wendell J, Rostgaard T, et al. Reduced volume but increased training intensity elevates muscle Na<sup>+</sup>-K<sup>+</sup> pump  $\alpha$ 1-subunit and NHE1 expression as well as short-term work capacity in humans. *Am J Physiol Regul Integr Comp Physiol* 2008;294:R966–74.
- [45] Juel C, Klarskov C, Nielsen JJ, Krstrup P, Mohr M, Bangsbo J. Effect of high-intensity intermittent training on lactate and H<sup>+</sup> release from human skeletal muscle. *Am J Physiol Endocrinol Metab* 2004;286:E245–51.